Received 20 October 1966 5.4, 5.18

Determination of Elastic and Piezoelectric Constants for Crystals in Class (3*m*)

A. W. Warner, M. Onoe,* and G. A. Coquin

Bell Telephone Laboratories, Incorporated, Murray Hill, New Jersey 07971

Determination of the elastic and piezoelectric constants for crystals in class (3*m*) is complicated by the large number of independent constants and the many possible ways in which they may be combined. An experimental and analytical procedure has been developed to determine all the constants using primarily thickness-mode measurements made on small, plate-shaped samples of various crystallographic orientations, and results using this procedure have been obtained for lithium tantalate and lithium niobate, two recently developed synthetic crystals. The resonant and antiresonant frequency constants for thickness modes have been calculated as functions of a plate's rotation angle. Information in this form makes possible the selection of plate orientations that might be useful as resonators and transducers.

INTRODUCTION

Recently, synthetic crystals in the class (3*m*) have attracted much interest because of their unusual combination of ferroelectric, optical, elastic, and piezoelectric properties. The successful application of these materials in ultrasonic devices, whether as resonators for electromechanical filter applications or as transducers in devices such as ultrasonic delay lines, depends upon a knowledge of the complete set of elastic, piezoelectric, and dielectric constants. The primary objectives of the present paper are: (1) to present a combination of experimental and analytical techniques that makes possible the determination of all the elastic and piezoelectric constants, and (2) to show how the constants may be used to calculate the fundamental resonant and antiresonant frequencies of a thickness-mode plate vibrator as a function of the plate orientation and from this information to predict plate orientations of maximum usefulness. The methods of this paper are applied specifically to two materials of technological importance, lithium tantalate, $LiTaO_3$, and lithium niobate, $LiNbO_3$.[1,2]

Most of the measurements involve thickness modes in plates. The use of thickness modes has the advantage that relatively small samples may be used and that the fabrication requirements are reduced to those of flatness, parallelism, and orientation of only the major faces of a sample. In principle it is possible to determine all the constants of materials in class (3*m*) by use of thickness modes, as has been done in the case of quartz, class (32), by Koga and Aruga.[3] However, the ferroelectric materials considered in this paper exhibited a slight nonuniformity when the same measurement was made on different samples of the same material. Since the thickness mode frequencies are not very sensitive to certain constants, in particular e_{31} and c_{13}^E, it was found necessary to make one additional measurement on a longitudinal mode resonator[4] to aid in the determination of these constants.

The symbols used in this paper will be in accordance with the IRE Standards on Piezoelectric Crystals, 1949 and 1958. The most frequently used symbols are listed below:

- c elastic constant (stiffness)
- c' piezoelectrically stiffened elastic constant
- $\bar{c}$ effective elastic constant (eigenvalue of Eq. 2)

* On leave of absence from Institute of Industrial Science University of Tokyo, Azabu, Tokyo, Japan.

[1] A. A. Ballman, "Growth of Piezoelectric and Ferroelectric Materials by the Czochralski Technique," J. Am. Ceramic Soc. **48**, p. 112–113 (1965).

[2] K. Nassau, H. J. Levinstein, and G. M. Lioacono, "Lithium Niobate I & II," J. Phys. Chem. Solids **27**, 983 and 989 (1966).

[3] I. Koga and M. Aruga, "Theory of Plane Elastic Waves in a Piezoelectric Crystalline Medium and Determination of Elastic and Piezoelectric Constants of Quartz," Phys. Rev. **109**, 1467–1473 (1958). Their form of piezoelectrically stiffened constants is somewhat different from Eq. 3. In the case of quartz, neglecting the difference between ϵ_{11} and ϵ_{33}, both formulas yield exactly the same results.

[4] W. P. Mason and H. Jaffe, "Methods for Measuring Piezoelectric, Elastic, and Dielectric Coefficients of Crystals and Ceramics," Proc. IRE **42**, 921–930 (1954).

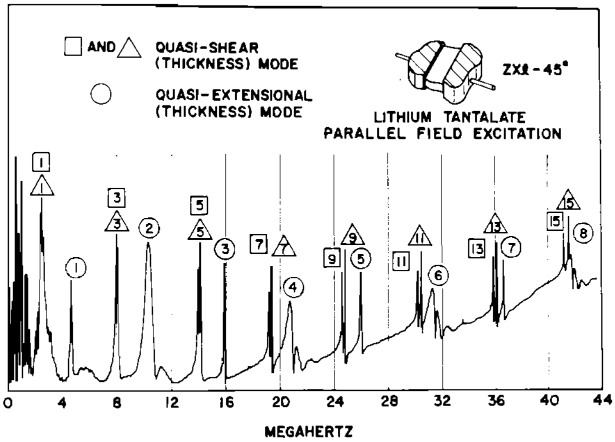

FIG. 1. Frequency spectrum of a rotated plate of lithium tantalate.

- e piezoelectric stress constant
- f frequency
- k electromechanical coupling factor
- m order of overtone
- $\mathbf{n}$ normal vector to a plate
- t thickness of a plate
- V phase velocity of elastic wave
- $\beta^{(\alpha)}$ eigenvector associated with $\bar{c}_\alpha$
- ϵ dielectric constant
- ρ density

I. REVIEW OF THICKNESS MODES OF VIBRATION

A thickness mode of vibration in a plate can be interpreted as a standing wave formed by waves propagating in a direction normal to the major surfaces. The velocity V_α of a plane wave in a piezoelectric medium propagating in the direction $\mathbf{n}$ is given by the following equation:

$$V_\alpha = (\bar{c}_\alpha/\rho)^{\frac{1}{2}}, \quad \alpha = 1, 2, 3, \tag{1}$$

where $\bar{c}_\alpha$ is an effective elastic constant, which is one of three eigenvalues of the following secular determinant:[5,6]

$$|c_{jk}' - \delta_{jk}\bar{c}| = 0, \tag{2}$$

in which c_{jk}' is a piezoelectrically stiffened elastic constant and is given by

$$c_{jk}' = [c_{ijkl}^E + (e_{pij}e_{qkl}n_pn_q)/(\epsilon_{rs}^S n_rn_s)]n_in_l. \tag{3}$$

If an effective elastic constant depends on any piezoelectric constants, it is called piezoelectrically stiffened, while, if it does not, it is called unstiffened.

Unit eigenvectors $\beta_k^{(\alpha)}$ associated with each eigenvalue $\bar{c}_\alpha$ give the directions of the displacement vectors of the three waves.

[5] A. W. Lawson, "The Vibration of Piezoelectric Plates," Phys. Rev. **62**, 71–76 (1942).
[6] H. F. Tiersten, "Thickness Vibrations of Piezoelectric Plates," J. Acoust. Soc. Am. **35**, 53–58 (1963).

The elastic wave motions existing in an electroded plate of a piezoelectric material are driven by an electric voltage applied to the electrodes. The determinantal equation for the resonant frequencies in the most general case, for a thickness-mode resonator excited by electrodes on the major surfaces, has been obtained by Tiersten[6] and is given as

$$|\beta_k^{(\alpha)}[c_{jk}'\gamma V_\alpha^{-1}\cos\gamma V_\alpha^{-1} - (e_{pij}e_{qkl}n_pn_qn_in_l)(\epsilon_{rs}n_rn_s)^{-1}\sin\gamma V_\alpha^{-1}]| = 0, \tag{4}$$

in which

$$\gamma = \pi f t. \tag{5}$$

The insertion of a root back into one of the minor determinants of Eq. 4 yields the amplitude ratios of the waves contributing to the resonance. This determinantal equation is very complicated in general. For high overtones, however, Eq. 4 is closely approximated by

$$\cos\gamma V_\alpha^{-1} = 0. \tag{6}$$

This simplification results because γ is very large and appears only in the coefficient of the cosine term. Consequently, the use of high overtones is much preferred over the use of fundamental or low overtones for the purpose of determining the constants. It should also be noted that, while Eq. 6 is an approximation for the high overtone resonant frequencies, it is exact for the antiresonant frequencies of the fundamental as well as the overtone modes. On the other hand, the resonant frequencies for the first few resonances are shifted to lower values than those given by the above equation.[6,7] However, because in a high overtone the difference between the resonant and the antiresonant frequency is small, the measurement of resonance instead of the more difficult measurement of antiresonance can safely be used.

Only stiffened waves can be excited when the electrodes are placed on the major surfaces. In this paper, this type of excitation is called perpendicular-field excitation. The unstiffened waves cannot be excited by the use of perpendicular-field excitation. On the other hand, some of them can be excited by a field parallel to the major surfaces. Such a field can be provided by placing the electrodes on the side (or minor) faces of a plate. This is called parallel-field excitation.[8] For this type of excitation, the resonant frequencies are given exactly by Eq. 6. There is no frequency shift due to piezoelectric boundary conditions on the major surfaces even in the low order resonances. However, the effects of contour configuration on resonant frequencies are still noticeable in low order resonances. Hence the use of high order resonances is again preferable.

[7] M. Onoe, H. F. Tiersten, and A. H. Meitzler, "Shift in the Location of Resonant Frequencies caused by Large Electromechanical Coupling in Thickness-mode Resonators," J. Acoust. Soc. Am. **35**, 36–42 (1963).
[8] A. W. Warner, "Use of Parallel Field Excitation in the Design of Quartz Crystal Units," Proc. 17th Freq. Control Symp., 248–266 (1963).

Equations 1 and 6 yield

$$\bar{c}_\alpha = 4\rho(f_m^{(\alpha)}t/m)^2, \tag{7}$$

where $f_m^{(\alpha)}$ is the frequency of the mth overtone. Thus, in the most general case, three effective elastic constants for any given orientation may be obtained experimentally, since there are in general three independent wave motions with different phase velocities. The measurement of a series of high order resonances is recommended to obtain a positive identification of any one mode sequence by checking the harmonic relationship, and improved accuracy can be obtained by averaging of the data. The nature of these resonances and their overtones is illustrated in Fig. 1, which is actually an experimental plot of the resonances in a rotated Y-cut plate of lithium tantalate. The three distinct series of overtones are evident, along with resonances associated with the edge dimensions. The highest overtone modes are very close to the values of antiresonance. The resonances at lower overtones may differ from this value depending on the value of the electromechanical coupling factor, on whether parallel- or perpendicular-field excitation is used, and on the ratio of the diameter to thickness dimensions of the plate. Although in principle any kind of plate orientation can be used, orientations that yield unstiffened modes are preferable, since the actual determination of the constants is simpler.

II. THICKNESS MODES FOR CRYSTAL PLATES IN CLASS (3m)

In the crystal class $(3m)$, there are six independent elastic, four independent piezoelectric, and two independent dielectric constants, as shown in the elasto-piezo-dielectric matrix in Fig. 2. An examination of the secular determinant in Eq. 2 for this case reveals that several plate orientations yield at least one unstiffened mode.

A Z-cut, Fig. 3(a), yields two unstiffened pure shear modes with the same frequency constants, and one stiffened pure extensional mode. Any electric field direction parallel to the major surface can excite the unstiffened modes. An X-cut, Fig. 3(b), yields one unstiffened pure extensional mode and two stiffened shear modes. Any field direction parallel to the major surface can excite the unstiffened mode.

A rotated Y-cut, Fig. 3(d), which includes a Y-cut, Fig. 3(c), as a special case, yields one unstiffened pure shear mode and two stiffened modes, which are mixtures of shear and extensional motions. A field along the X axis excites the unstiffened mode and a field along Z' axis excites the remaining two stiffened modes. Hence an electrode configuration that gives only the field parallel to X axes is preferred because the identification of modes becomes simple. If the identification is not a problem, then the parallel-field electrodes may be rotated around the Y' or thickness axis, so that all three modes can be excited simultaneously with only one electrode configuration, as is the case in Fig. 1.

$$\left|\begin{array}{cccccc|ccc}
c_{11} & c_{12} & c_{13} & c_{14} & 0 & 0 & 0 & -e_{22} & e_{31} \\
c_{12} & c_{11} & c_{13} & -c_{14} & 0 & 0 & 0 & e_{22} & e_{31} \\
c_{13} & c_{13} & c_{33} & 0 & 0 & 0 & 0 & 0 & e_{33} \\
c_{14} & -c_{14} & 0 & c_{44} & 0 & 0 & 0 & e_{15} & 0 \\
0 & 0 & 0 & 0 & c_{44} & c_{14} & e_{15} & 0 & 0 \\
0 & 0 & 0 & 0 & c_{14} & c_{66} & -e_{22} & 0 & 0 \\
\hline
0 & 0 & 0 & 0 & e_{15} & -e_{22} & \epsilon_{11} & 0 & 0 \\
-e_{22} & e_{22} & 0 & e_{15} & 0 & 0 & 0 & \epsilon_{11} & 0 \\
e_{31} & e_{31} & e_{33} & 0 & 0 & 0 & 0 & 0 & \epsilon_{33}
\end{array}\right|$$

where $(c_{11}-c_{12})=2c_{66}$. The superscripts, such as c^E and ϵ^S, are omitted.

FIG. 2. Elasto-piezo-dielectric matrix for the crystal class $(3m)$.

III. PROCEDURES FOR DETERMINING CONSTANTS

Dielectric constants can be obtained from capacitance measurement of plates with full electrodes. At frequencies well above any of the strong resonances, the constant ϵ_{33}^S is obtained from a Z-cut and ϵ_{11}^S from either an X-cut or a Y-cut. At very low frequencies, well below any strong resonances, the constants ϵ_{33}^T and ϵ_{11}^T are obtained. Although the constants ϵ_{33}^S and ϵ_{11}^S are the ones needed to obtain the piezoelectric stress constants, the constants ϵ_{33}^T and ϵ_{11}^T can be determined much more accurately from low-frequency capacitance measurements. To circumvent this problem, the experimental values for ϵ_{33}^S and ϵ_{11}^S were used to obtain tentative values of the piezoelectric constants, and later all constants were readjusted slightly to fit the measured values of ϵ_{33}^T and ϵ_{11}^T.

Parallel-field excitation of unstiffened modes, as mentioned in the previous Section, immediately yields the following constants: c_{44}^E from a Z-cut, c_{11}^E from an X-cut, c_{66}^E from a Y-cut, and c_{14}^E from a rotated Y-cut.

Since the stiffened mode in a Z-cut is a pure extensional mode, the electromechanical coupling factor $k_t=(e_{33}^2/c_{33}'\epsilon_{33}^S)^{\frac{1}{2}}$ can be obtained from the ratios of measured fundamental and overtone resonant frequencies.[7] This is the only fundamental thickness-mode resonant frequency needed for the measurement of the constants, so special selection of a large Z-cut plate free from unwanted resonances is desirable. The constants c_{33}^E and e_{33} are obtained from k_t and the measured effective elastic constant $\bar{c}_3$ by the following equations:

$$c_{33}^E = (1-k_t^2)\bar{c}_3, \tag{8}$$

$$e_{33} = [\epsilon_{33}^S \bar{c}_3 k_t^2]^{\frac{1}{2}}. \tag{9}$$

The sign of e_{33} must be chosen so that the piezoelectric strain constant d_{33} is positive, as specified by the IRE standard on piezoelectric crystals. This usually, although not necessarily, implies that e_{33} is positive.

(a) Z-cut

$$\begin{vmatrix} c_{44}-\bar{c} & 0 & 0 \\ 0 & c_{44}-\bar{c} & 0 \\ 0 & 0 & c_{33}+\beta_{33}e_{33}^2-\bar{c} \end{vmatrix}=0$$

(b) X-cut

$$\begin{vmatrix} c_{11}-\bar{c} & 0 & 0 \\ 0 & c_{66}+\beta_{11}e_{22}^2-\bar{c} & c_{14}-\beta_{11}e_{15}e_{22} \\ 0 & c_{14}-\beta_{11}e_{15}e_{22} & c_{44}+\beta_{11}e_{15}^2-\bar{c} \end{vmatrix}=0$$

(c) Y-cut

$$\begin{vmatrix} c_{66}-\bar{c} & 0 & 0 \\ 0 & c_{11}+\beta_{11}e_{22}^2-\bar{c} & -(c_{14}-\beta_{11}e_{15}e_{22}) \\ 0 & -(c_{14}-\beta_{11}e_{15}e_{22}) & c_{44}+\beta_{11}e_{15}^2-\bar{c} \end{vmatrix}=0$$

(d) Rotated Y-cut (around X-axis)

$$\begin{vmatrix} L & 0 & 0 \\ 0 & M'-\bar{c} & F' \\ 0 & F' & N'-\bar{c} \end{vmatrix}=0$$

where

$$\begin{aligned} L&=m^2c_{66}+n^2c_{44}+2mnc_{14} \\ M'&=m^2c_{11}+n^2c_{44}-2mnc_{14}+\beta(mne_{15}+m^2e_{22}+mne_{31})^2 \\ N'&=m^2c_{44}+n^2c_{33}+\beta(m^2e_{15}+n^2e_{33})^2 \\ F'&=mn(c_{13}+c_{44})-m^2c_{14}+\beta(mne_{15}+m^2e_{22}+mne_{31})(m^2e_{15}+n^2e_{33}) \\ \beta&=(m^2\epsilon_{11}+n^2\epsilon_{33})^{-1} \end{aligned}$$

FIG. 3. Secular determinants for plate orientations yielding unstiffened modes (a) Z-cut, (b) X-cut, (c) Y-cut, and (d) rotated Y-cut (around X axis).

The perpendicular-field excitation of a Y-cut yields two effective elastic constants, $\bar{c}_2$ and $\bar{c}_3$.[9] Since they are roots of the secular determinant shown in Fig. 3(c), the following equations hold:

$$\Sigma_Y=(\bar{c}_2+\bar{c}_3)_Y=c_{11}^E+c_{44}^E+\beta_{11}^S(e_{15}^2+e_{22}^2), \tag{10}$$

$$\Pi_Y=(\bar{c}_2\cdot\bar{c}_3)_Y=c_{11}^Ec_{14}^E-(c_{14}^E)^2+c_{11}^E\beta_{11}^Se_{15}^2 +c_{44}^E\beta_{11}^Se_{22}^2+2c_{14}^E\beta_{11}^Se_{15}e_{22}. \tag{11}$$

Similarly, the perpendicular-field excitation of an X-cut also yields two effective elastic constants, and from Fig. 3(b) they must satisfy the following:

$$\Sigma_X=(\bar{c}_2+\bar{c}_3)_X=c_{44}^E+c_{66}^E+\beta_{11}^S(e_{15}^2+e_{22}^2), \tag{12}$$

$$\Pi_X=(\bar{c}_2\cdot\bar{c}_3)_X=c_{44}^Ec_{66}^E-(c_{14}^E)^2+c_{66}^E\beta_{11}^Se_{15}^2 +c_{44}^E\beta_{11}^Se_{22}^2+2c_{14}^E\beta_{11}^Se_{15}e_{22}. \tag{13}$$

By a careful rearrangement of Eqs. 10–13, we find that

$$c_{44}^E+\beta_{11}^Se_{15}^2=(\Pi_Y-\Pi_X)/(\Sigma_Y-\Sigma_X), \tag{14}$$

$$c_{66}^E+\beta_{11}^Se_{22}^2=\Sigma_X-(\Pi_Y-\Pi_X)/(\Sigma_Y-\Sigma_X), \tag{15}$$

$$c_{11}^E+\beta_{11}^Se_{22}^2=\Sigma_Y-(\Pi_Y-\Pi_X)/(\Sigma_Y-\Sigma_X), \tag{16}$$

$$(c_{14}^E+\beta_{11}^Se_{15}e_{22})^2=[(\Sigma_Y-\Sigma_X)(\Pi_Y\Sigma_X-\Pi_X\Sigma_Y) -(\Pi_Y-\Pi_X)^2]/(\Sigma_Y-\Sigma_X)^2. \tag{17}$$

Thus, since all constants appearing in Eqs. 14–17 other than e_{15} and e_{22} are known, we can determine the magnitude of e_{15} from Eq. 14, the magnitude of e_{22} from both Eqs. 15 and 16, and the relative sign between e_{15} and e_{22} from Eq. 17. The absolute signs of e_{15} and e_{22} are selected so that the piezoelectric strain constant d_{22} is positive. That is,

$$d_{22}=e_{22}(s_{11}^E-s_{12}^E)-e_{15}s_{14}^E>0, \tag{18}$$

according to the IRE convention. Notice that Eqs. 14–17 provide four equations to solve for only two unknowns, so that any inconsistencies in the measurements are immediately apparent.

Perpendicular-field excitation of a rotated Y-cut yields two effective elastic constants. From Fig. 3 their sum is expressed by the following equation:

$$(\bar{c}_2+\bar{c}_3)_{Y'}=M'+N', \tag{19}$$

in which all constants except e_{31} are known. Since Eq. 19 is a quadratic equation for e_{31}, selection of the proper value for e_{31} can in principle be made by comparing the values obtained from two different rotated Y-cuts.

Unfortunately the values of e_{31} obtained from Eq. 19 are extremely sensitive to the measured values of $\bar{c}_2$ and $\bar{c}_3$, and small errors in these effective elastic constants can lead to fairly large errors in e_{31}. Hence it is desirable to measure some quantity that depends more strongly on e_{31}, and such a quantity is the coupling factor k_{31} of a rectangular bar with its length along the X axis and with electrodes applied to the Z faces. When the length of the bar is much larger than the transverse dimensions, the coupling factor k_{31} is approximately given by

$$k_{31}=(d_{31}^2/\epsilon_{33}^Ts_{11}^E)^{\frac{1}{2}}. \tag{20}$$

The sign of d_{31} can be determined by a static test, and since s_{11}^E can be found from the fundamental resonant frequency of the bar, d_{31} can be calculated from Eq. 20. Then the equation

$$e_{31}=d_{31}[c_{11}^E+c_{12}^E-2(c_{13}^E)^2/c_{33}^E]+c_{13}^Ee_{33}/c_{33}^E \tag{21}$$

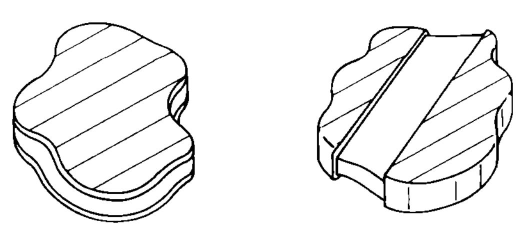

PERPENDICULAR FIELD (a) PARALLEL FIELD (b)

FIG. 4. Electrode configurations for (a) a perpendicular-field excitation, and (b) a parallel-field excitation.

[9] This $\bar{c}_3$ is, of course, different from the one obtained from a Z-cut in the previous section. When it is necessary, the orientation of a plate will be identified in the following manner: $(\bar{c}_3)_Y$ and $(\bar{c}_3)_Z$, etc.

provides a relation between the two remaining unknown constants e_{31} and c_{13}^E.

The magnitude of c_{13}^E can be found from the value of s_{11}^E found from the bar measurement, with the sign of c_{13}^E selected to give agreement with the effective elastic constants measured on a rotated Y-cut plate. Alternatively, c_{13}^E can be selected to give the best fit to measurements made on several different rotated Y-cut plates and in this way obtain a check on the consistency of the data.

IV. EXPERIMENTAL TECHNIQUES

The plates used in the experiments were irregular in shape and averaged in area about 0.25 cm². The small size is a consequence of using small, experimentally grown boules of crystalline material. The ability to use such plates is of course a distinct advantage in the evaluation of new materials. Every effort was made to produce flat, parallel plates so that the thickness dimension would have significance to at least three figures. In practice, the thickness ranged from 0.200 to 1.000 mm with thickness variations in a given plate less than 0.0005 mm ($\frac{1}{2}\ \mu$). The thicker plates could be operated on high overtones, while the thinner plates gave better freedom from unwanted modes at the fundamental and low overtone modes.

The electrodes used were gold, deposited directly on the crystal plates by evaporation in a vacuum of about 10^{-4} torr. Figure 4 shows the electrode configuration for perpendicular- and parallel-field excitation.

The perpendicular-field plates were clamped directly in a Wayne–Kerr 1–100-MHz admittance bridge to minimize lead inductance, while the parallel-field plates were held in the bridge by miniature spring clips. In some instances, where a desired resonance was extremely weak, additional sensitivity was obtained by the use of a hybrid transformer bridge such as is used to evaluate unwanted resonances in quartz filter plates. The admittance bridge is, of course, more desirable because of its better definition of the series resonance.

The use of a sweep oscillator was found to be extremely useful in sorting out the many resonances in any one plate, as well as in selecting a frequency free from resonances for the measurement of capacitance. An extreme example is shown in Fig. 1 where even and odd overtones of the thickness extensional mode and the odd overtones of both thickness shear modes can

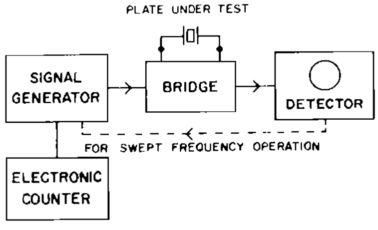

Fig. 5. System for measuring resonant frequencies.

Table I. Constants of lithium tantalate.

Density	ρ	7.45×10^3 kg/m³		
Dielectric constants	$\epsilon_{11}^S/\epsilon_0$	41	$\epsilon_{11}^T/\epsilon_0$	51
	$\epsilon_{33}^S/\epsilon_0$	43	$\epsilon_{33}^T/\epsilon_0$	45
Elastic constants	c_{11}^E	2.33×10^{11} N/m²	c_{11}^D	2.39×10^{11} N/m²
	c_{12}^E	0.47	c_{12}^D	0.41
	c_{13}^E	0.80	c_{13}^D	0.80
	c_{14}^E	−0.11	c_{14}^D	−0.22
	c_{33}^E	2.75	c_{33}^D	2.84
	c_{44}^E	0.94	c_{44}^D	1.13
	c_{66}^E	0.93	c_{66}^D	0.99
Piezoelectric constants	e_{15}	2.6 C/m²	d_{15}	2.6×10^{-11} C/N
	e_{22}	1.6	d_{22}	0.7
	e_{31}	0.0	d_{31}	−0.2
	e_{33}	1.9	d_{33}	0.8
	β_{11}^S	2.8×10^9 m/F	β_{11}^T	2.2×10^9 m/F
	β_{33}^S	2.6	β_{33}^T	2.5
	s_{11}^E	4.87×10^{-12} m²/N	s_{11}^D	4.76×10^{-12} m²/N
	s_{12}^E	−0.58	s_{12}^D	−0.50
	s_{13}^E	−1.25	s_{13}^D	−1.20
	s_{14}^E	0.64	s_{14}^D	1.02
	s_{33}^E	4.36	s_{33}^D	4.19
	s_{44}^E	10.8	s_{44}^D	9.3
	s_{66}^E	10.9	s_{66}^D	10.5
	g_{15}	5.8×10^{-2} m²/C	h_{15}	7.2×10^9 N/C
	g_{22}	1.5	h_{22}	4.3
	g_{31}	−0.6	h_{31}	0.0
	g_{33}	2.1	h_{33}	5.0

be identified. It can further be seen that some estimate of coupling and Q can be made as well as an identification of the several series of resonances.

Figure 5 shows the schematic diagram of the system for measuring the series resonant frequencies of a plate. The sweep oscillator is continuously variable as to sweep width, sweep rate, and center frequency. Crystal controlled harmonic markers are provided every 1, 2, 5, or 10 MHz. It is usually sufficient in the measurement of any one resonance to set the sweep for a narrow range of frequency, set sweep rate to manual, find the peak or null depending on which bridge is in use, and read the frequency on a frequency counter. If greater precision is desirable, a frequency synthesizer may be substituted for the sweep oscillator, and a tuned voltmeter for the detector. The system covers from 50 KHz to 100 MHz, and since the fundamental resonance of a plate may be near 3 MHz, overtones as high as 30 can be measured.

The accuracy of determining the frequency constant from overtones is about ±0.1%, limited principally by the thickness measurement. Since values from a number of plates of lithium tantalate of the same orientation show variations as high as 1%, particularly when different boules or crystals are involved, it is believed that imperfections in domain structure[10] are significant in this measurement.

[10] R. L. Barns, "X-ray Powder Data, Density and Precision Lattice Parameters of Lithium Tantalate, $LiTaO_3$" (to be published).

TABLE II. Comparison between measured and calculated frequency constants of lithium tantalate (unit: hertz-meter).

	Unstiffened		Stiffened							
			Antiresonance		Resonance		Antiresonance		Resonance	
	mes.	cal.	mes.	cal.	mes.	cal.	mes.	cal.	mes.	cal.
X	2800	2798	2093	2078	1906	1906	1680	1670	...	1665
Y	1760	1767	2854	2857	2801	2811	1911	1913	1822	1793
Z	1775	1776	3086	3092	3040	3049	...	...	...	...
Rotated Y 25°	1693	1686	3117	3106	2959	2979	1684	1700	...	1679
45°	1670	1664	3176	3158	3080	3047	1686	1710	...	1709
120°	1868	1862	3043	3058	3043	3000	1663	1674	1663	1673
135°	1871	1873	2937	2974	2931	2918	1743	1721	...	1700
170°	...	1802	2785	2775	2765	2768	1986	1977	1834	1830

V. DETERMINATION OF CONSTANTS FOR LITHIUM TANTALATE

Single domain crystals of lithium tantalate, $LiTaO_3$, are grown by the Czochralski technique.[1] X-, Y- and Z-cuts as well as several rotated Y-cuts are fabricated and the orientations are checked by x-ray methods.[10]

The procedures from the first three paragraphs in Sec. III are straightforward. The coupling factor k_t of the Z-cut plate is 19%. In the procedure of the fourth paragraph the following results were obtained for e_{15} and e_{22} from Eqs. 14–17:

$$e_{15}^2 = 6.8(\mathrm{C/m^2})^2$$
$$e_{22}^2 = 3.1$$
$$e_{22}^2 = 2.1$$
$$e_{15}e_{22} = +4.1$$

The above results show a fair amount of inconsistency and the values $e_{15}=2.6$ and $e_{22}=1.6$ were selected as a compromise fit. In the procedure of the sixth paragraph of Sec. III the coupling factor k_{31} was found to be 8%, and the value $d_{31}=-0.2\times10^{-11}$ C/N is obtained from this. When the value of c_{13}^E found by the procedure of the seventh paragraph is used, the value of e_{31} calculated from Eq. 21 is $e_{31}=0.0$ to two significant figures. This does not at all imply that e_{31} is exactly equal to zero.

The results are summarized in Table I. With these constants, it is possible to calculate the frequency constants of the fundamental resonances from Eq. 5 for plates of any orientation. Table II shows the comparison between measured and calculated frequency constants for the fundamental antiresonance (high order resonance) and resonance of various cuts. Good experimental accuracy for the fundamental resonance should not be expected because of the small size of the plates. In some instances the fundamental resonance could not be measured due to interference of other modes. The agreement between measured and calculated frequency constants seen in Table II is reasonably good, with discrepancies less than 1% in most cases. Figures 6–8 show the variation of frequency constants of the fundamental resonances and antiresonances of a lithium-tantalate plate, when it is excited by a perpendicular field, as functions of rotation angle of a plate around the X, Y, and Z axes, respectively. The separation between the resonance and antiresonance of a stiffened mode is a measure of the strength of a mode. The figures show no such separation for an unstiffened mode, because it is not excited by a perpendicular field.

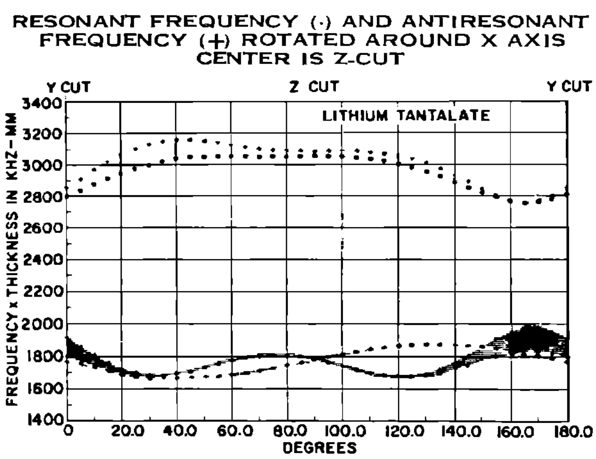

FIG. 6. Frequency constants of the fundamental resonances and antiresonances of a $LiTaO_3$ plate rotated around the X axis (rotated Y-cut).

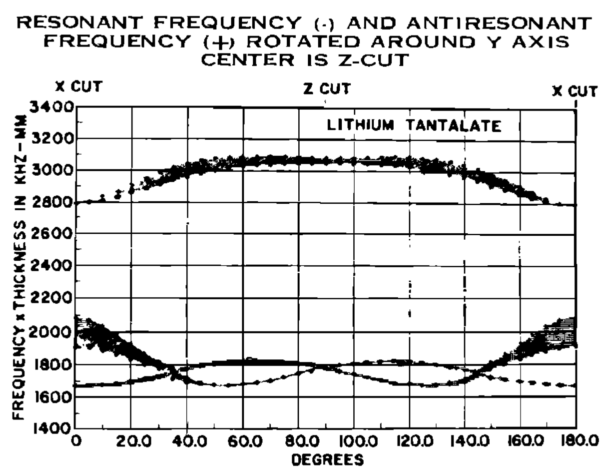

FIG. 7. Frequency constants of the fundamental resonances and antiresonances of a $LiTaO_3$ plate rotated around the Y axis.

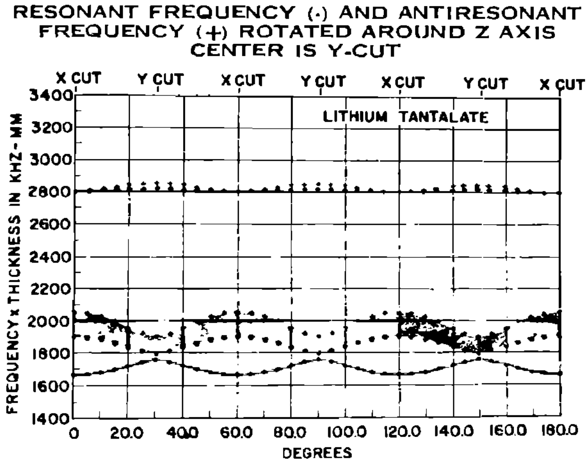

FIG. 8. Frequency constants of the fundamental resonances and antiresonances of a $LiTaO_3$ plate rotated around the Z axis.

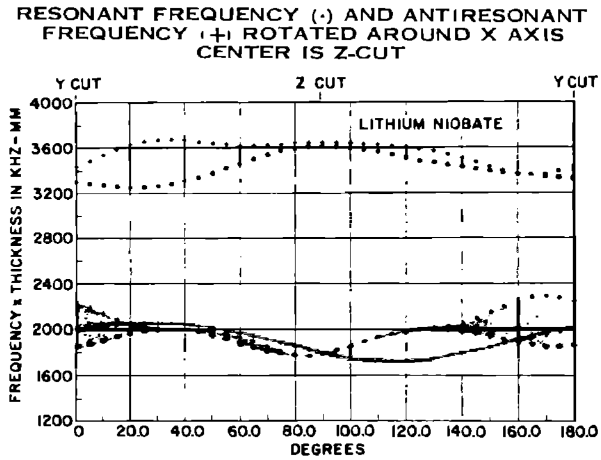

FIG. 10. Frequency constants of the fundamental resonances and antiresonances of a $LiNbO_3$ plate rotated around the X axis (rotated Y-cut).

We can define an effective coupling factor for a mode in terms of the separation between the fundamental resonance and antiresonance as follows:

$$k_{\mathrm{eff}}=\left[\left(\frac{\pi}{2}\frac{f_{\mathrm{R}}}{f_{\mathrm{A}}}\right)\Big/\tan\left(\frac{\pi}{2}\frac{f_{\mathrm{R}}}{f_{\mathrm{A}}}\right)\right]^{\frac{1}{2}}, \qquad (22)$$

where f_{R} and f_{A} are the resonant and antiresonant frequencies, respectively. This definition is equivalent to the usual definition of coupling factor when there is only one stiffened mode.[7] The effective coupling factors of the quasishear and quasiextensional modes of a rotated Y-cut plate are plotted in Fig. 9 as functions of the angle of rotation. Also plotted in Fig. 9 is the angle φ between the extensional wave displacement vector and the plate normal. Since the displacement of the unstiffened shear wave is always along the X axis, φ is also the angle the stiffened shear wave displacement makes with the plane of the plate.

For transducer applications it is advantageous to have a high effective coupling factor, but in addition it is often required that only one wave, extensional or shear, be excited. Referring to Fig. 9, we can see that for the 165° rotated Y-cut plate the effective coupling factor of the quasiextensional mode vanishes whereas the effective coupling factor of the quasishear mode has a high value of 41%. Also the angle φ is nearly zero so that the mode of vibration is nearly a pure mode. Hence this cut would make an excellent shear wave transducer. Similarly, the 47° cut has a quasiextensional mode coupling of 29% and no coupling to the quasishear mode. The angle φ for this cut is 1.4° which, although not as small as for the 165° cut, is small enough so that this cut could be used as an extensional wave transducer for most applications. The 111° cut also has no coupling to the quasishear mode, but $\varphi=-2.6°$ for this cut, and this is too large to permit use as a transducer because an excessive amount of shear wave would be excited. Of course the Z-cut, with a coupling factor of 19%,

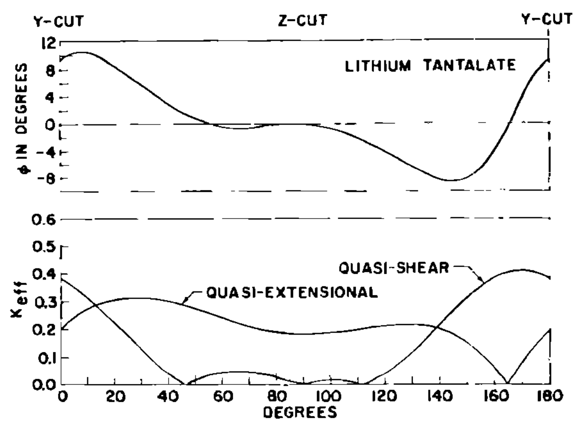

FIG. 9. Effective coupling factors and angle φ between quasi-extensional wave displacement and plate normal for rotated Y-cuts of $LiTaO_3$.

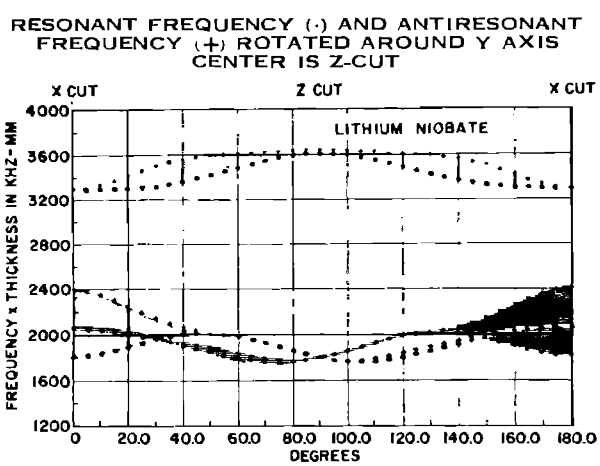

FIG. 11. Frequency constants of the fundamental resonances and antiresonances of a $LiNbO_3$ plate rotated around the Y axis.

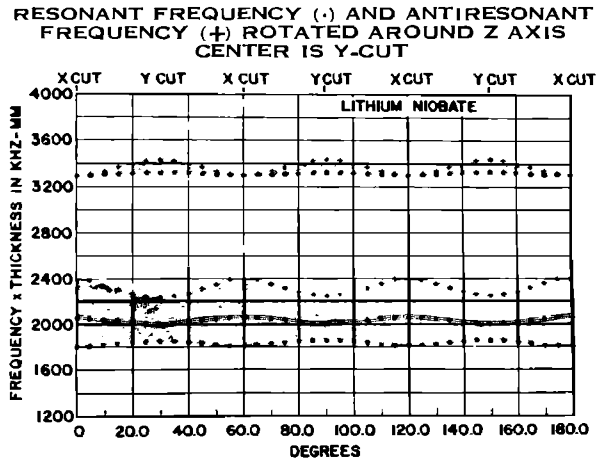

FIG. 12. Frequency constants of the fundamental resonances and antiresonances of a $LiNbO_3$ plate rotated around the Z axis.

could also be used as an extensional wave transducer. All of the cuts mentioned above could be used for resonator applications, since in that case the purity of the mode of vibration is immaterial. Notice that in all cases the effective coupling factor goes to zero linearly with the angle of rotation rather than quadratically. This implies that the mode whose effective coupling goes to zero is excited with opposite phase in rotated Y-cuts with angles on either side of the angle at which the effective coupling is zero.

Another interesting point, which can be observed in Figs. 7 or 8, is that one of the stiffened shear modes in an X-cut plate is very weak. The other shear mode is quite strong with an effective coupling factor of 44%. An X-cut plate used as a transducer would excite one shear wave in the delay medium very strongly and the other shear wave would be weakly excited. Since the two shear waves in an isotropic delay medium are degenerate, this is not objectionable. Thus the X-cut plate, because of its high effective coupling factor, might be the best choice for a shear wave transducer on an isotropic delay medium.

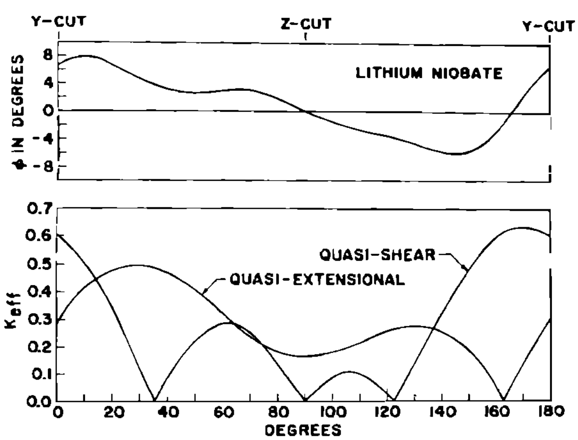

FIG. 13. Effective coupling factors and angle φ between quasi-extensional wave displacement and plate normal for rotated Y-cuts of $LiNbO_3$.

TABLE III. Constants of lithium niobate.

Density	ρ	4.7×10^3 kg/m³		
Relative Dielectric constants	$\epsilon_{11}^S/\epsilon_0$	44	$\epsilon_{11}^T/\epsilon_0$	84
	$\epsilon_{33}^S/\epsilon_0$	29	$\epsilon_{33}^T/\epsilon_0$	30
Elastic constants	c_{11}^E	2.03×10^{11} N/m²	c_{11}^D	2.19×10^{11} N/m²
	c_{12}^E	0.53	c_{12}^D	0.37
	c_{13}^E	0.75	c_{13}^D	0.76
	c_{14}^E	0.09	c_{14}^D	−0.15
	c_{33}^E	2.45	c_{33}^D	2.52
	c_{44}^E	0.60	c_{44}^D	0.95
	c_{66}^E	0.75	c_{66}^D	0.91
Piezoelectric constants	e_{15}	3.7 C/m²	d_{15}	6.8×10^{-11} C/N
	e_{22}	2.5	d_{22}	2.1
	e_{31}	0.2	d_{31}	−0.1
	e_{33}	1.3	d_{33}	0.6
	β_{11}^S	2.6×10^9 m/F	β_{11}^T	1.34×10^9 m/F
	β_{33}^S	3.9	β_{33}^T	3.8
	s_{11}^E	5.78×10^{-12} m²/N	s_{11}^D	5.20
	s_{12}^E	−1.01	s_{12}^D	−0.44
	s_{13}^E	−1.47	s_{13}^D	−1.45
	s_{14}^E	−1.02	s_{14}^D	0.87
	s_{33}^E	5.02	s_{33}^D	4.89
	s_{44}^E	17.0	s_{44}^D	10.8
	s_{66}^E	13.6	s_{66}^D	11.3
	g_{15}	9.1×10^{-2} m²/C	h_{15}	9.5×10^9 N/C
	g_{22}	2.8	h_{22}	6.4
	g_{31}	−0.4	h_{31}	0.8
	g_{33}	2.3	h_{33}	5.1

VI. DETERMINATION OF CONSTANTS FOR LITHIUM NIOBATE

In determining the constants of lithium niobate by the procedure discussed in Section III, the coupling factor k_t of the Z-cut plate was found to be 17%. No inconsistencies were found when using the procedure of the fourth paragraph, Sec. III, to find e_{15} and e_{22}. The coupling factor k_{31} in the procedure of the fifth paragraph was found to be 2%. The results are summarized in Table III. Table IV shows the comparison between measured and calculated frequency constants for the fundamental antiresonance (high order resonance) and resonance of various cuts. Figures 10 to 12 show the variation of frequency constants as functions of rotation angle of a plate around the X, Y, and Z axes, respectively.

The effective coupling factors of the quasiextensional and quasishear modes of a rotated Y-cut plate are shown in Fig. 13 as is the angle φ between the quasi-extensional wave displacement vector and the plate normal. The 163° rotated Y-cut plate has zero coupling to the quasiextensional mode. The angle φ for this cut is only −1.6° so that it can be used as a shear wave transducer, and the effective coupling factor of the quasishear mode is 62%, which is remarkably high for a single-crystal, high Curie temperature material. Both the 36° and 123° rotated cuts have zero coupling to the

TABLE IV. Comparison between measured and calculated frequency constants of lithium niobate (unit: hertz-meter).

	Unstiffened		Stiffened							
			Antiresonance		Resonance		Antiresonance		Resonance	
	mes.	cal.	mes.	cal.	mes.	cal.	mes.	cal.	mes.	cal.
X	3290	3289	2405	2397	2049	2051	2032	2037	1838	1803
Y	1993	1993	3425	3430	3297	3306	2239	2231	1868	1845
Z	1788	1788	3660	3659	3615	3620	...	1788	...	1788
Rotated Y 45°	2012	2015	3692	3661	3303	3342	2023	1994	2005	1976
60°	1942	1950	3664	3629	3415	3467	1933	1935	1900	1871
135°	1750	1763	3531	3542	3458	3436	2067	2041	2052	1999
160°	...	1891	...	3366	...	3363	2276	2244	1896	1869

quasishear wave, but the angle φ in both cases is too large for these cuts to be useful for transducers, and only the Z-cut is suitable for an extensional wave transducer.

As in the case of lithium tantalate, one of the stiffened shear modes in an X-cut plate is very weak. The other shear mode in this case has an effective coupling factor of 68%, thus the X-cut would make an excellent shear wave transducer on an isotropic delay medium. It can be seen in Figs. 10 and 11 that the frequency constants of the weak shear mode lie between the resonance and antiresonance of the strong shear mode. This causes the interesting phenomenon of the weak mode having an antiresonance lower in frequency than its resonant frequency, since it is obvious that a crystal cannot have two resonances without an intermediate antiresonance.

VII. CONCLUSION

A method for determining all the elastic and the piezoelectric constants of a crystal in the class ($3m$) has been discussed. By making use primarily of resonant frequencies of high overtones in thin plates, this method allows the use of rather small crystals.

The constants of lithium niobate and lithium tantalate have been determined. The variation of frequency constants of the fundamental resonance as well as antiresonance have been calculated as functions of rotation angle around the X, Y, and Z axes, so that useful cuts may be selected. Several cuts of both materials, and in particular lithium niobate because of its very high effective coupling factors, appear to be useful for transducer applications.

ACKNOWLEDGMENTS

The work represented by this paper would not have been possible without the close cooperation of A. A. Ballman, K. Nassau, R. L. Barns, and others who made available materials and data in the early stages of development of lithium tantalate and lithium niobate. T. B. Bateman kindly made available some of his plane wave measurements on lithium niobate for comparison. Some serious errors in an earlier version of this work (presented at the IEEE Sonics and Ultrasonics Symposium, Cleveland, October 1966) were pointed out by R. T. Smith and resulted in this present revised paper. In addition, the authors take pleasure in acknowledging valuable criticisms and suggestions received from A. H. Meitzler and H. F. Tiersten.